Journal of Applied Electrochemistry **33**: 933–937, 2003.

Catalytic epoxidation with electrochemically *in situ* generated hydrogen peroxide☆

ANDREAS ZIMMER[1,*], DAMIAN MÖNTER[2] and WLADIMIR RESCHETILOWSKI[1]
[1]*Institut für Technische Chemie, Technische Universität Dresden, Dresden, Germany*
[2]*Tricat Zeolites GmbH, Bitterfeld, Germany*
*(*author for correspondence, e-mail: andreas.zimmer@chemie.tu-dresden.de)*

Received 12 November 2002; accepted in revised form 1 July 2003

Key words: electrocatalysis, epoxidation, hydrogen peroxide, silicalite, trickle-bed electrode

Abstract

The epoxidation of allyl alcohol with *in situ* generated hydrogen peroxide was performed in an electrochemical cell with a trickle-bed electrode, composed of carbon black, graphite, PTFE and titanium silicalite-1 (TS-1) as heterogeneous epoxidation catalyst. Mass transport in interaction with the catalytic activity limits the epoxidation rate. The conversion of allyl alcohol increases with increase in the content of epoxidation catalyst in the electrode. In contrast, the specific reaction rate decreases due to the reduced accessibility of active sites in the catalyst.

1. Introduction

Epoxides are important key products in the chemical industry. At present, the widely used manufacturing processes, particularly for propylene oxide, are either environmentally critical (chlorohydrine process) or give rise to large amounts of byproducts (isobutanol or methylphenylcarbinol in case of the Oxirane process), Figure 1. Process modifications, designed to permit complete recycling of the reaction solvent in the chlorohydrine process by electrochemical regeneration are not currently utilized on an industrial scale [1, 2].

Catalytic reaction between the olefins and oxygen seems to be an ideal route, however it is only possible for the production of ethylene oxide. Up to now, epoxidations with hydrogen peroxide have failed on account of high cost and the absence of effective catalysts. Consequently, there is interest in the search for alternative, improved production routes for olefins. New developments are in progress, particularly to find effective catalysts for epoxidations with hydrogen peroxide.

In 1982 it was found that titanium silicalite 1 (TS-1), a crystalline, microporous molecular sieve with ZSM-5 structure containing up to 2.5 mol% of isomorphously silicon substituted titanium, has the potential to catalyse a variety of liquid phase oxidation reactions with hydrogen peroxide, e.g. the epoxidation of olefinic compounds or the hydroxylation of aromatics [3]:

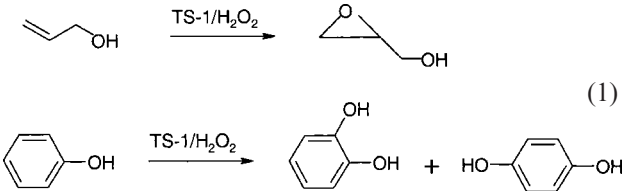

The technical advantage of this catalyst is simple. The separation from the reactants occurs by filtration, and only water is formed as by-product. Recently, Enichem (Italy) has built a pilot plant for the epoxidation of propylene to propylene oxide, in which the epoxidation system TS-1/H_2O_2 is used [4]. BASF (Germany) is looking for a site to build a large scale factory for this process in the near future [5].

In the case of propylene oxide, prices of raw materials (propylene 300 €/t and hydrogen peroxide 1000 €/t) are approximately 800 €/t propylene oxide. The price of propylene oxide is approximately 1000 €/t. Further production costs (catalysator, energy) and lower selectivity of the reaction, mean that a profitable production is unlikely.

Consequently, epoxidation processes are being investigated, which use less expensive oxidants as raw materials than hydrogen peroxide. The high selectivity of the TS-1 catalysed epoxidation reaction must be preserved. This can be expected, if, in the first reaction step, hydrogen peroxide is formed as intermediate, and reacts immediately with the olefin, catalysed by TS-1.

The formation of hydrogen peroxide from the cheap raw materials oxygen and hydrogen is used industrially

☆ This paper was originally presented at the 6th European Symposium on Electrochemical Engineering, Düsseldorf, Germany, September 2002.

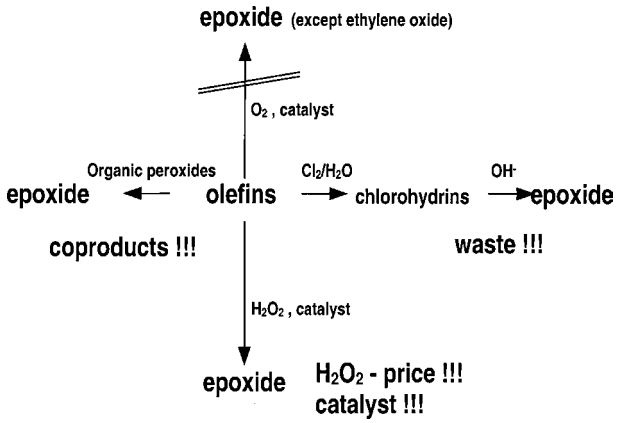

Fig. 1. Traditional and new routes to produce epoxides.

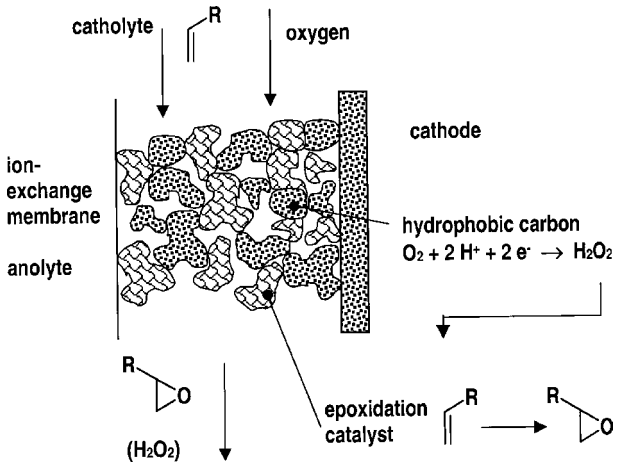

Fig. 2. Epoxidation with *in situ* generated hydrogen peroxide.

in the anthraquinone process. CLERICI [6] combined this reaction pathway with the TS-1 catalysed epoxidation of propylene to propylene oxide. The two reaction steps, the *in situ* formation of hydrogen peroxide and the epoxidation, occur to a great extent without mutual interference. The interaction of the anthraquinone/anthrahydroquinone redox system with the TS-1 is limited because of the small pore dimensions of the heterogenous catalyst. The yields are lower compared with the *ex situ* synthesis of propylene oxide by H_2O_2/TS-1.

The alternative combination of hydrogen peroxide formation by cathodic reduction of oxygen with TS-1 catalysed epoxidation has not been investigated up to the present. In this case the reaction system is very simple (see Figure 2). The two reaction steps, the electrochemical formation of hydrogen peroxide and the following epoxidation, occur in a catalytic mixture located in the form of porous particles in the cathodic chamber of an electrolytic cell. The reactants are supplied in the gas phase or dissolved in the electrolyte. Initially hydrogen peroxide formed on the carbon black particles reacts at the heterogenous TS-1 catalyst with the olefin. Besides the epoxide, water and oxygen (by anodic water decomposition) are formed.

Hydrophobic carbon black is the preferred electrode material for the cathodic hydrogen peroxide formation [7]. In these experiments, trickle bed electrodes are used [8–10], because of their simple form and high space-time yield. Compared to parallel plate electrodes, a considerably greater electrode surface is formed. The intergranular void volume offers sufficient space for the flow of electrolyte and gas without affecting pressure drop.

2. Experimental

2.1. *Materials and working conditions*

To characterize the epoxidation activity of TS-1, many investigations have been performed with allyl alcohol to produce glycidol (2,3-epoxy-1-propanol) [11, 12], see Equation 1. Therefore, the study of catalytic epoxidation in this work was performed with allyl alcohol as model substrate. The cell used for electrochemical–catalytic epoxidation is shown in Figure 3. The cell consisted of two compartments separated by an ion exchange membrane NAFION 417 (Du Pont). A titanium anode, coated with a RuO_2/TiO_2 layer was used (DSA, Heraeus).

The cathode composite consisted of granular particles of graphite coated with a catalytic active layer of a mixture of carbon black, PTFE and TS-1. The cathode was 0.6 cm thick and had a geometric area of 15 cm^2. The void fraction of the electrode was approximately 0.5. Glass spherules were used to achieve a homogeneous distribution of gas and electrolyte over the cross section of the cathode. In the trickle bed, the individual particles were visible as shown in Figure 4(a). Figure 4(b) shows a schematic view of the cross section of a particle.

The materials used and the composition are listed in Table 1. The graphite particles and the carbon black were acid washed to remove heavy metal impurities. The preparation of the coated particles occurred by mixing all the components in an aqueous suspension. The suspension was transferred to a rotary evaporator and the water was stripped off at 80 °C under vacuum. The

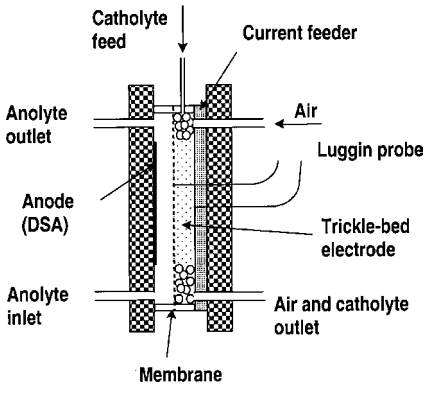

Fig. 3. Schematic diagram of the electrolytic cell.

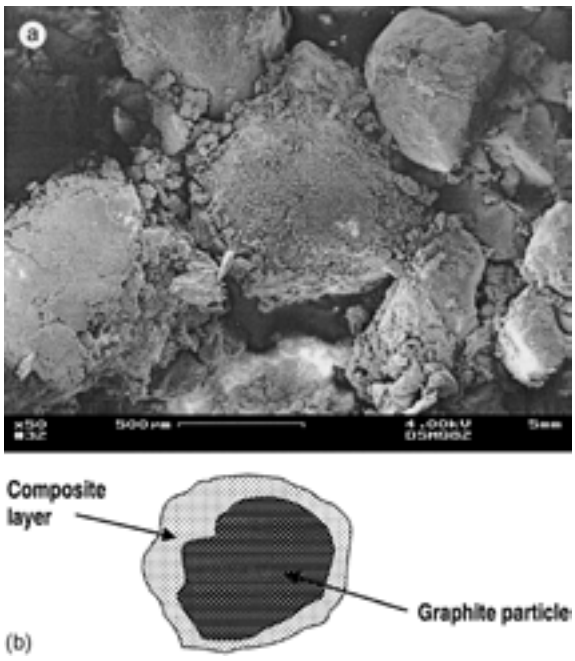

Fig. 4. Structure of the trickle-bed electrode and the individual particles. (a) Structure of the trickle-bed electrode (SEM, 50×). (b) Schematic cross section of a coated particle.

Table 1. Components and composition of the electrode material

Component	Amount in the electrode material /%	Amount in the electrocatalytic active layer of the electrode material /%
Graphite particle[a]	75–90	–
PTFE[b]	3.2–8.0	12.7–37.6
Carbon black[c]	9.4–32	37.5–84
TS-1[d]	0–12.5	0–50

[a] common electrode graphite, mean particle diameter 1 mm.
[b] high surface acetylene black as P1042, Stickstoffwerk Piesteritz, Germany.
[c] used as suspension, Dyneon TF5032.
[d] Degussa.

composite was tempered at 300 °C for 2 h to obtain the electrocatalytic activity for hydrogen peroxide formation.

Figure 5 shows the distribution of the TS-1-crystals in the carbon black matrix for a composite with 50 wt.% TS-1 in the catalytic active layer. The TS-1 crystals are partially agglomerated.

The catholyte (0.1 mol l^{-1} Na_2SO_4 as supporting electrolyte) and oxygen (air) were supplied from the top of the cathode compartment. The anolyte was recirculated over a thermostated storage tank. All experiments were carried out at a temperature of 25 °C. The investigations related to hydrogen peroxide formation were performed in a single pass mode, the epoxidation experiments in a recirculation mode. The electrolysis was carried out by using the constant current method.

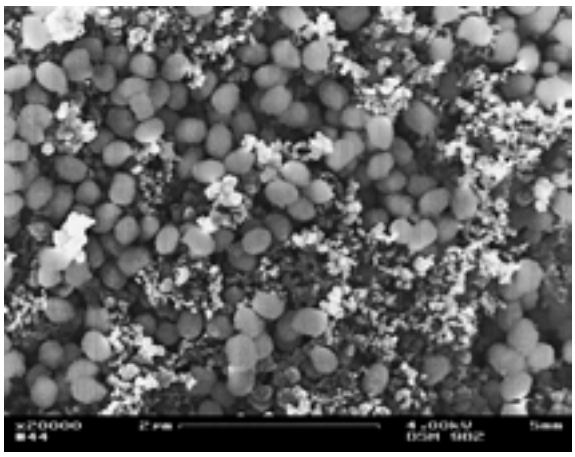

Fig. 5. Composite of the electrocatalytic active layer (SEM, 20 000×), TS-1 crystals (light grey grains) in PTFE-bounded carbon black matrix.

Cathode potentials were registered against the SCE without ohmic correction. The Luggin capillaries were positioned in the trickle bed cathode near the current feeder and at the membrane, respectively.

2.2. *Analytical conditions*

GC analysis of allyl alcohol and epoxidation products were performed by a HP 6890 system with autosampler on a cyclodextrine capillary column (Lipodex A, Macherey-Nagel). The electrolyte samples were added with an internal standard (dimethoxyethane) and injected without further preparation.

The concentration of hydrogen peroxide was recorded by an ampereometric sensor (Dulcometer PEROX, ProMinent) and controlled by permanganat titration. During epoxidation experiments control measurements were performed by standard iodometric titration.

The results such as current yield of hydrogen peroxide, allyl alcohol conversion and glycidol yield were calculated from the experimental values.

3. Results and discussion

3.1. *Hydrogen peroxide formation*

Figure 6 shows the current density/potential plots during the reduction of oxygen in the trickle bed cathode. The form of the curves is similar at all investigated electrode materials which had electrocatalytic activity for hydrogen peroxide formation. The two Luggin capillaries are positioned at the current feeder and at the membrane, respectively. At each Luggin capillary, the upper curve shows the overall current density, the lower curve the hydrogen peroxide reaction current density. With the measurement of the hydrogen peroxide concentration in every operating steady state at the overall current density, the current yield α_{HP} for hydrogen peroxide was calculated from the hydrogen

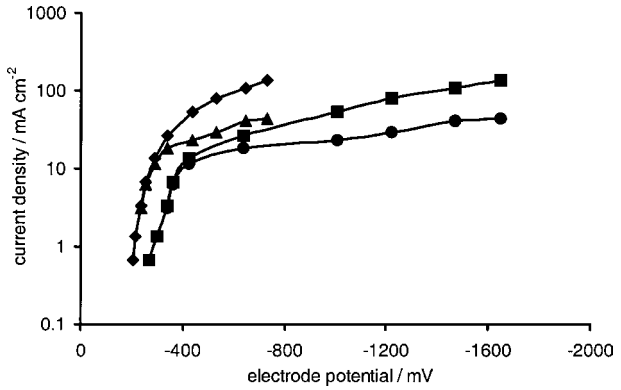

Fig. 6. Current density–potential plot at the trickle bed electrode during hydrogen peroxide formation, air 5 l h^{-1}, electrolyte 1 l h^{-1}, 0.1 mol l^{-1} Na_2SO_4, electrode material ARP50TS, cf. Table 2, position of the luggin tip: (–♦–) electrode, overall current; (–■–) membrane, overall current; (–▲–) electrode, hydrogen peroxide reaction current; (–●–) membrane, hydrogen peroxide reaction current.

peroxide concentration C_{HP}, the current density i and the volumetric flow rate of the electrolyte $\dot{v}$:

$$i_{HP} = \frac{C_{HP}\dot{v}A}{i}zF$$

A is the geometric area of the cathode. The hydrogen peroxide reaction current density i_{HP} is calculated from:

$$I_{HP} = i\alpha_{HP}$$

The current density/potential curves at the current feeder and at the membrane differ considerably. At the current feeder, the potentials are less negative, compared with the membrane. The potential distribution over the thickness of the trickle bed results from the different conductivity of the electrode material and the electrolyte–gas mixture in the void volume of the electrode [13]. Only small potential differences arise at low current densities. The whole electrode works in the potential range between −200 and −400 mV vs SCE, which is favourable for the hydrogen peroxide formation. The current yields reach values of more than 80% at current densities less then 20 mA cm^{-2} (cf. Figure 7). Especially at high current densities, large potential differences were found between the two measuring points. Very negative potentials arise near the membrane. Consequently, side reactions such as the reduction of oxygen to water or the formation of hydrogen may occur. These side reactions reduce the current yield of hydrogen peroxide formation. This is shown in Figure 6 by the enhanced difference between the values of the overall current density and the hydrogen peroxide reaction current density at potentials more negative then −400 mV vs SCE.

The form of the current density/potential curves suggests activation controlled processes at current densities lower than 10 mA cm^{-2}. At higher current densities, the electrode processes take place under diffusion control. The mass transfer limitation can result by the

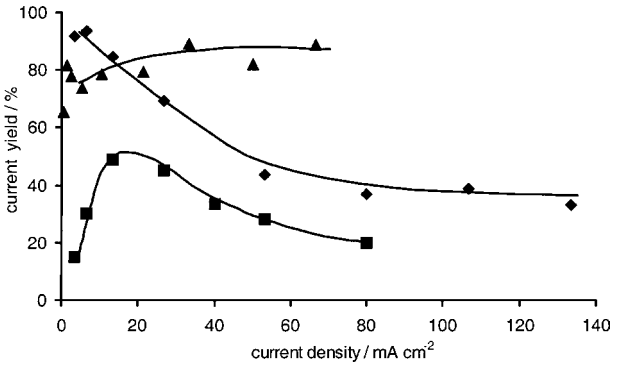

Fig. 7. Current yield of hydrogen peroxide vs overall current density at different electrode materials, air 5 l h^{-1}, electrolyte 1 l h^{-1}, 0.1 mol l^{-1} Na_2SO_4, electrode material: (–♦–) acetylene black with 50% TS-1 (ARP50TS); (–■–) carbon black without TS-1; (–▲–) acetylene black without TS-1.

slow transfer of oxygen from the gas phase into the liquid phase.

Increasing the current density, the differences between the overall current and the hydrogen peroxide reaction current become higher. This is represented by plotting the current yield against the current density at cathodes which contain different electrode components and compositions (Figure 7). The best results have been found with acetylene black in the electrocatalytic active layer without epoxidation catalyst. With carbon black from other sources (furnace black) only low current yields are obtained. High contents of TS-1 (ARP50TS with 50 wt.% TS-1) lead to a significant decrease of hydrogen peroxide current yield especially at high current densities.

3.2. *Epoxidation*

Figure 8 shows the concentration/time curves of the electrochemical–catalytic epoxidation of allyl alcohol. The electrolysis was carried out with catholyte recirculation. At the beginning of the electrolysis the hydrogen peroxide concentration in the electrolyte was zero. The epoxidation reaction was started by applying a high

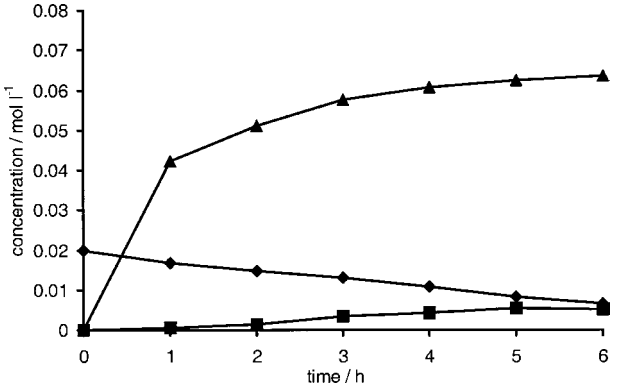

Fig. 8. Concentration–time plot, electrochemical epoxidation of allyl alcohol, electrode material with 50 wt.%TS-1 (ARP50TS), air 5 l h^{-1}, electrolyte 1 l h^{-1}, 0.1 mol l^{-1} Na_2SO_4. (–♦–) Allyl alcohol; (–■–) glycidol; (–▲–) hydrogen peroxide.

Table 2. Electrochemical epoxidation with different composition (TS-1 content) of the electrocatalytic active material, recirculation mode, electrolyte with 0.1 mol l^{-1} Na_2SO_4, 0.02 mol l^{-1} allyl alcohol, 25 °C, conversion and yield after 3 h reaction time

Electrode material	Amount of TS-1 in the electrocatalytic active material /%	Conversion allyl alcohol /%	Yield glycidol /%	k_1 /h^{-1}	k_{eff} /h^{-1} g^{-1}
ARP12TS	12	21.9	5.7	0.081	0.479
ARP25TS	25	30.8	18.6	0.117	0.345
ARP50TS	50	34.1	17.7	0.137	0.156

current of 0.8 A (53 mA cm^{-2}) for the first hour. In this time a strong growth of the hydrogen peroxide concentration in the recirculated electrolyte was observed. The current was reduced to 0.2 A (13 mA cm^{-2}) to guarantee a relatively constant level of hydrogen peroxide. The course of the reaction is visible in decreasing allyl alcohol concentration and increasing glycidol concentration. The concentration of hydrogen peroxide increases slowly for the next 2 h and remains nearly constant afterwards. In Table 2 the degree of conversion for allyl alcohol and the yield for glycidol are given after 3 h of reaction. The yield loss of glycidol may be attributed to consecutive reactions to glycerol and glycerol derivatives. The rate constants in Table 2 refer to reaction 1.

With increasing content of TS-1 in the catalytic active layer the pseudo-first-order rate constant k_1 becomes higher. In contrast, the mass specific rate constant k_{eff} decreases. This relationship was not expected and is not easy to understand. Regarding the reaction scheme (Figure 2) and the electrode structure (Figure 5) short mass transport routes were expected between the locations of the hydrogen peroxide formation (carbon black particles) and the epoxidation (TS-1 crystals). With a sufficient rate of hydrogen peroxide formation, this should result in a epoxidation rate, which is defined by the rate constant k_1 and the mass of the catalyst. In accordance with the reaction kinetics, an increasing mass of TS-1 must increase the epoxidation rate. In contrast, the results in Table 2 shows that the growth of the rate constant k_1 is clearly below the growth of the catalyst mass. The specific rate constant k_{eff} even shows a significant decrease. This influence may be caused by the distribution of TS-1 in the carbon black/PTFE matrix. At low content the crystals of TS-1 are homogenously distributed within the electrode material. With increasing TS-1 content the distribution becomes different, and with 50 wt.% TS-1 in the material a significant part is agglomerated (cf. Figure 5). The hydrogen peroxide, formed at the carbon black particles, has a longer diffusion path to the active sites of the TS-1. This results in a stronger reaction inhibition for the epoxidation.

3.3. *Conclusions*

Using oxygen as oxidizing agent, the epoxidation of allyl alcohol has been shown to be possible in a single step. The process occurs with hydrogen peroxide formed as an intermediate in an electrochemical trickle-bed reactor.

The process is limited by mass transport and the catalytic activity of the epoxidation catalyst. Expected synergistic effects by arrangement of the reaction centers in microscopic dimensions could not be verified with the electrode material used. The composition of the electrode material and the operating conditions have a large influence on hydrogen peroxide generation. With increasing amount of TS-1 in the electrode material and increasing current density the reaction conditions for the hydrogen peroxide formation deteriorate. High percentage of TS-1 in the electrode material causes a drop of catalytic activity.

With further development of the manufacturing process and the composition of the electrocatalytic active material new interesting results are to be expected.

Acknowledgements

The authors gratefully acknowledge financial support of this work by the Arbeitsgemeinschaft industrieller Forschungsvereinigungen (AiF).

References

1. K.H. Simmrock, *Hydrocarbon Process* **57** (1978) 105.
2. D. Kahlich, U. Wiechern and J. Lindner, *in* 'Ullmann's Encyclopedia of Industrial Chemistry' (Web Edition, WILEY-VCH, 2002).
3. C. Perego, A. Carati, P. Ingallina, M.A. Mantegazza and G. Bellussi, *Appl. Catalysis A* **221** (2001) 63.
4. E. Occhiello, *Chemistry and Industry* (1997) 761.
5. C. Schierloh, *Nachr. Chemie* **50** (2002) 809.
6. M.G. Clerici and P. Ingallina, *Catal. Today* **41** (1998) 351.
7. O. Spaleka and J. Balej, *Coll. Czech. Chem. Commun.* **46** (1981) 2052.
8. D. Pletcher, *Acta Chem. Scand.* **53** (1999) 745.
9. P.C. Foller and R.T. Bombard, *J. Appl. Electrochem.* **25** (1995) 613.
10. N. Yamada, T. Yaguchi, H. Otsuka and M. Sudoh, *J. Electrochem. Soc.* **146** (1999) 2587.
11 M.G. Clerici and P. Ingallina, *J. Catal.* **140** (1993) 71.
12. D. Mönter, Dissertation TU Dresden, Shaker-Verlag, Aachen 2002.
13. D. Pletcher and F.C. Walsh, 'Industrial Electrochemistry' (Blackie Academic & Professional, Glasgow, 1993), p. 129.